ISBN: 978-3-95450-261-5 ISSN: 2673-7000 doi: 10.18429/JACoW-NAPAC2025-THP040

GROWTH AND CHARACTERIZATION OF GAAS-BASED SPIN-POLARIZED PHOTOCATHODES*

P. Saha†, L. Cultrera, M. Boukhicha, T. Tsang, L. Lathpandura, R. Bagy, J. Walsh
Brookhaven National Laboratory, Upton, NY, USA
A. Muhowski, S. Hawkins, V. Patel
Sandia National Laboratories, Albuquerque, NM, USA

Abstract

Spin-polarized electron sources find application in both high-energy and nuclear physics experiments. We describe in detail the design and characterization of different photocathodes based on GaAs/GaAsP superlattice structures. These structures are fabricated with a Distributed Bragg Reflector (DBR) aimed at achieving a high quantum efficiency (QE) ~20% in addition to a high electron spin polarization (ESP) ~85% at the desired wavelength of 780 nm. We present the QE and ESP measurements of photoemitted electrons as a function of wavelength of incident light, along with morphological and photoluminescence measurements.

INTRODUCTION

Spin-polarized electron sources play a critical role in various fields of fundamental physics research, be it nuclear physics or high-energy physics. Examples include the study of nuclear structure, understanding the dynamics of strong interactions, and electro-weak nuclear physics [1].

Historically, bulk GaAs with high quantum efficiency (QE) and moderately high electron spin polarization (ESP) of the order of 35-40% (theoretically the maximum possible ESP 50%), was used as a source of spin-polarized electrons [2]. Strained GaAs-based photocathodes were developed to lift the degeneracy of the heavy-hole (hh) and light-hole (lh) valence bands, which was limiting the ESP to a maximum of 50% in bulk GaAs. The strained photocathodes yielded a higher ESP, but the QE was low due to the low thickness of the samples used to prevent any strain relaxation [3]. To circumvent the problem of low QE and strain relaxation, strain-compensated superlattice (SL) structures based on AlGaAs/GaAs, GaAs/GaAsP, AlInGaAs/GaAsP, InGaAs/AlGaAs, GaAsSb/AlGaAs were designed which were fabricated with a Distributed Bragg Reflector (DBR) [4, 5]. The SL structures leverage the use of quantum wells (QWs) and quantum barriers (QBs) to further increase the hh-lh band splitting while the use of DBR enhances QE by increasing optical absorption through multiple photon passes within the resonant cavity.

* The work is supported by Brookhaven Science Associates, LLC under Contract DE-SC0012704 with the U.S. DOE. Sandia National Laboratories is a multimission laboratory managed and operated by National Technology & Engineering Solutions of Sandia, LLC, a wholly owned subsidiary of Honeywell International Inc., for the U.S. Department of Energy's National Nuclear Security Administration under contract DE-NA0003525.
† psaha3@bnl.gov

To meet the requirements of the different applications of spin-polarized electron sources for example, the Electron-ion collider, International Linear Collider etc, it is critical to push the performance limits of the sources than the existing cathodes in terms of QE and ESP. In this paper, we discuss our effort to design, grow and characterize GaAs/GaAsP based spin-polarized photocathodes to generate electron beam with a high QE and a high ESP simultaneously.

DESIGN AND GROWTH OF PHOTOCATHODE STRUCTURES

The strain-compensated superlattice (SL) photocathodes were grown via the Molecular Beam Epitaxy (MBE) technique at Sandia National Laboratories. These structures were designed to accommodate a large number of GaAs QWs and GaAsP QBs, which enables the production of electrons with both high ESP and QE [6].

The photocathode structure is similar to that reported in the previous works [7], except in the choice of the Fabry–Pérot spacer layer. In the present structure, a nominally 290 nm thick tuning layer $Al_{0.15}Ga_{0.85}As_{0.81}P_{0.19}$ was grown as the Fabry–Pérot spacer instead of $GaAs_{0.81}P_{0.19}$. AlGaAsP was selected for its higher band gap energy, which suppresses electron excitation from this layer within the target wavelength range, thereby preventing dilution of the ESP from unwanted electron contributions.

Material	Thickness (nm)	Doping level (cm^{-3})	
GaAs	4	$p = 3 \times 10^{19}$	
$GaAs_{0.62}P_{0.38}$	3.85	$p = 5 \times 10^{17}$	30 pairs
GaAs	3.85	$p = 5 \times 10^{17}$	
$Al_{0.15}Ga_{0.85}As_{0.81}P_{0.19}$	290	$p = 1 \times 10^{18}$	
$AlAs_{0.78}P_{0.22}$	58	$p = 1 \times 10^{18}$	10 pairs
$GaAs_{0.81}P_{0.19}$	65	$p = 1 \times 10^{18}$	
$GaAs_{0.81}P_{0.19}$	2000	$p = 1 \times 10^{18}$	
GaAs -> $GaAs_{0.81}P_{0.19}$	2750	$p = 1 \times 10^{18}$	
GaAs buffer	200	$p = 1 \times 10^{18}$	
GaAs substrate		$p > 1 \times 10^{18}$	

Figure 1: Schematic of the SL-DBR GaAs/GaAsP photocathode. The GaAs surface layer was capped with amorphous As at the end of the epitaxial growth to prevent any surface contamination.

Figure 1 shows the schematic representation of the complete photocathode structure, consisting of the substrate, DBR, and superlattice layer with a heavily doped final layer

ISBN: 978-3-95450-261-5 ISSN: 2673-7000 doi: 10.18429/JACoW-NAPAC2025-THP040

of GaAs. The GaAs surface layer was capped with amorphous arsenic at the end of the epitaxial growth process to prevent any surface contamination and/or oxidation.

Figure 2 shows the photoluminescence (PL) spectrum measured from SL-DBR photocathode using a 355 nm UV laser. A strong emission peak was observed at around 782 nm with a full width at half maximum (FWHM) of 20 nm.

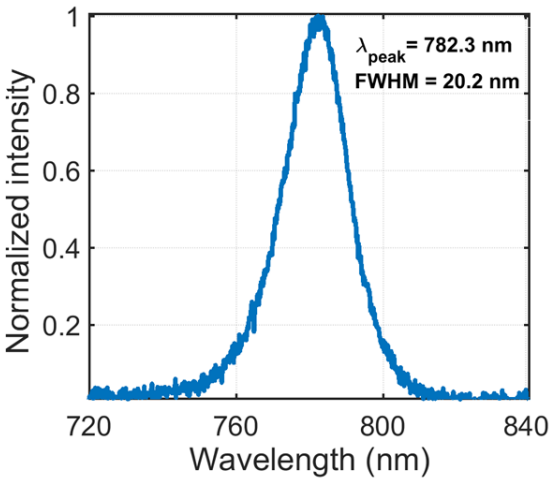

Figure 2: Photoluminescence spectrum measured from the GaAs/GaAsP superlattice photocathode showing a prominent emission peak at 782 nm with a FWHM of 20.2 nm.

NEA ACTIVATION

The cathode was heat cleaned at 450 °C to remove the arsenic cap and allowed to cool to room temperature radiatively. Once at room temperature, the cathode was exposed to Cs vapor and oxygen (introduced through a leak valve into the chamber) in alternate cycles, by the commonly used technique known as the 'yo-yo' method. During the activation process, the QE from the sample illuminated with photons at 530 nm was monitored. A 20 V negative bias was applied to the sample with respect to the walls of the chamber to extract the photoelectrons, which was measured using a lock-in amplifier. Each cycle involved alternating exposure to cesium (Cs) and oxygen (O_2). During the Cs exposure, the sample was deliberately over-cesiated, causing the photocurrent to decrease to 65% of its peak value. Subsequent exposure to an O_2 flux led to a rise in photocurrent. The sample was exposed to O_2 flux till the photocurrent attained a peak and then reduced to 80% of its peak value.

Figure 3 shows the temporal evolution of QE from the GaAs/GaAsP photocathode upon illumination with photons at 530 nm during the 1st activation process. A final QE of 15% was obtained at 530 nm at the end of the activation.

The cathode was characterized for QE and ESP measurements following the first NEA activation, as detailed in the subsequent sections. A second NEA activation was performed after heat cleaning the sample, followed by another set of QE and ESP measurements.

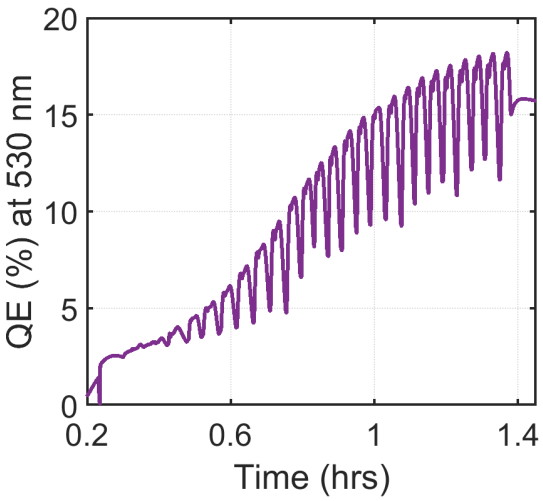

Figure 3: Activation of photocathode sample to the NEA condition via "yo-yo" technique. The final QE measured from the cathode was ~15% at 530 nm.

QE SPECTRAL RESPONSE

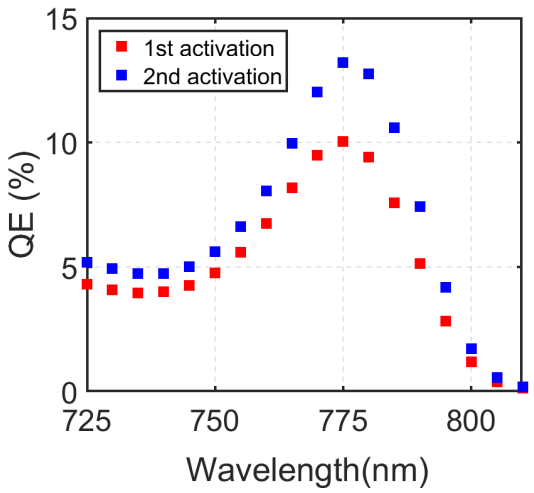

Figure 4: QE measured from sample GaAs/$GaAs_{0.62}P_{0.38}$ (3.85/3.85 nm X 30 layer pairs) as a function of illumination wavelength. A maximum QE of ~10% was observed at 775 nm after the first activation, while it was measured to be ~13% at 775 nm after the second activation process.

The quantum efficiency from the SL-DBR photocathode was measured after each NEA activation as a function of incident light wavelength. The cathode was illuminated with light from a tungsten halogen lamp (Oriel Model #66088) coupled with a monochromator (Oriel Cornerstone Model #130). Figure 4 represents the spectral response of QE from the photocathode upon illumination with photons in the wavelength range 725-810 nm measured directly after NEA activation. A maximum QE of ~10% and ~13% was measured at a wavelength of 775 nm due to the first and second activation cycles, respectively.

ISBN: 978-3-95450-261-5 ISSN: 2673-7000 doi: 10.18429/JACoW-NAPAC2025-THP040

ESP MEASUREMENT

The electron spin polarization measurements require the use of circularly polarized light obtained by using a combination of a linear polarizer (Thorlabs Model # LPVIS050) and a tunable liquid crystal retarder LCR (Thorlabs Model # LC1113B) to generate spin-polarized electrons. The LCR can switch the handedness of circular polarization.

The electron beam generated from the photocathode biased at -200 V with respect to the chamber walls is longitudinally spin-polarized. The electron beam was bent by 90 degrees via an electrostatic bend to obtain transversely polarized beam. The transversely polarized electron beam was collimated and steered towards the gold thin film (target) via a series of electrostatic elements. By carefully optimizing and tuning the electrostatic voltages, a transport efficiency of ~25% was achieved in deflecting the electrons from the photocathode to the gold target (biased at positive 25 kV). The beam, upon entering the retarding-field Mott polarimeter, is accelerated due to a 25 kV potential difference between the inner and outer hemispheres. The beam then scatters off the gold surface at 25 kV, is decelerated back to the transport energy of 200 eV as it exits the inner hemisphere/electrode, and goes back towards the outer electrode. [4] Scattered electrons that have the kinetic energy to overcome the retarding field are detected by two symmetrically placed channel electron multipliers (channeltrons) [8].

The electron spin polarization is calculated by dividing the measured asymmetry between left and right scattering by the effective Sherman function S_{eff}, which has been calibrated to be 0.125 using a standard commercially available bulk GaAs wafer. The data acquisition and analysis were performed using LabVIEW programming software.

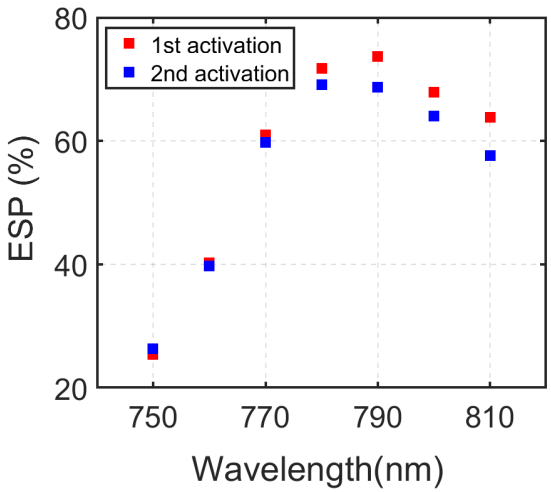

Figure 5: ESP as a function of the incident light wavelength (750-810 nm) measured from the SL-DBR photocathode.

Figure 5 shows the ESP measured from the GaAs/GaAsP photocathode as a function of the incident wavelength between 750 - 810 nm. A maximum ESP of 73% was observed at 790 nm during the first activation. The maximum ESP measured was slightly lower at 70% after the second activation cycle, probably due to the formation of a thicker/complete NEA layer (confirmed by higher QE) and a larger number of scattering sites, leading to depolarization of emitted electrons.

One of the reasons limiting the ESP of the photoemitted electrons to a slighly lower value than the target 80-85% may be due to the origin of trench defects during the growth process as seen in Fig. 6. The figure shows the surface morphology of the photocathode measured using a laser microscope (Keyence Model # VK-X1100) under a magnification of 20X and 150X. The trench defects may act as scattering sites for the emitted electrons, thereby randomizing their spin orientation leading to a reduced ESP. The cause of the trench defects is currently being investigated by performing TEM measurements on the samples to identify the specific layer of the photocathode structure at which these defects nucleate.

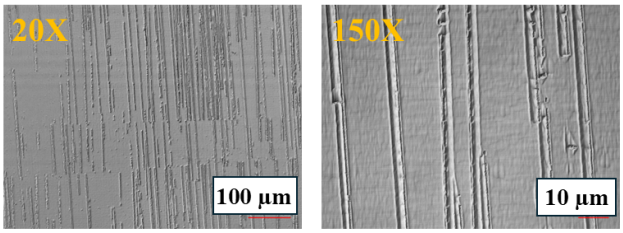

Figure 6: Surface morphology map of the SL-DBR photocathode measured using a Keyence laser microscope with a magnification of 20X and 150X, respectively, indicates the formation of trench defects.

CONCLUSION AND FUTURE STEPS

In this paper, we discussed the growth and characterization of an MBE-grown GaAs/GaAsP-based SL-DBR photocathode with AlGaAsP as a Fabry–Pérot spacer layer. The photocathode yielded a maximum QE of ~13% at 775 nm and a maximum ESP of ~73% at 790 nm.

Future work will involve further efforts to optimize the design of the GaAs/GaAsP strained superlattice structure in terms of concentration and thickness of the different layers, aiming to achieve a higher splitting between the hh-lh minibands and to facilitate the fabrication of an ideal photocathode structure with a high ESP and QE at the desired wavelength. ESP measurements from the photocathodes will be performed by cryogenically cooling the cathodes to liquid nitrogen temperatures.

We plan to focus our attention on the design, optimization, and growth of the following superlattice structures directly on GaAs, which may yield a higher ESP:

1. GaAsP/ InGaAs operated at 800 nm,
2. GaAsP/ GaAsSb operated at 1030 nm.

ISBN: 978-3-95450-261-5 ISSN: 2673-7000 doi: 10.18429/JACoW-NAPAC2025-THP040

REFERENCES

[1] H. Montgomery, "Jefferson lab: A long decade of physics", *J. Phys. Conf. Ser.*, vol. 299, p. 011001, Apr. 2011. doi:10.1088/1742-6596/299/1/011001

[2] D.T. Pierce *et al.*, "The GaAs spin polarized electron source", *Rev. Sci. Instrum.*, vol. 51, pp. 478-499, 1980. doi:10.1063/1.1136250

[3] T. Maruyama *et al.*, "Observation of strain-enhanced electron spin polarization in photoemission from InGaAs", *Phys. Rev. Lett*, vol. 66, p. 2376, 1991. doi:10.1103/PhysRevLett.66.2376

[4] W. Liu *et al.*, "Evaluation of GaAsSb/AlGaAs strained superlattice photocathodes", *AIP Advances*., vol. 8, p. 075308, 2018. doi:10.1063/1.5040593

[5] T. Maruyama *et al.*, "Systematic study of polarized electron emission from strained GaAs/ GaAsP superlattice photocathodes", *Appl. Phys. Lett.*, vol. 85, pp.2640–2642, 2004. doi:10.1063/1.1795358

[6] J. Biswas *et al.*, "Record quantum efficiency from strain compensated superlattice GaAs/GaAsP photocathode for spin polarized electron source", *AIP Advances*, vol. 13, p. 085106, 2023. doi:10.1063/5.0159183

[7] L. Cultrera, A. Muhowski, M. Boukhicha, P. Saha, S. Hawkins, and V. Patel, "Development of spin polarized electron sources based on III-V semiconductors at BNL", in *Proc. IPAC'24*, Nashville, TN, USA, May 2024, pp. 2064–2067. doi:10.18429/JACoW-IPAC2024-WEPC46

[8] T. Gay and F.B. Dunning, "Mott electron polarimetry", *Rev. Sci. Instrum.*, vol. 63, p.1635–1651, 1992. doi:10.1063/1.1143371